Cell

Sites of Regulated Phosphorylation that Control K-Cl Cotransporter Activity

Jesse Rinehart,[1,5] Yelena D. Maksimova,[2] Jessica E. Tanis,[3] Kathryn L. Stone,[5,6] Caleb A. Hodson,[1] Junhui Zhang,[1] Mary Risinger,[7] Weijun Pan,[4] Dianqing Wu,[4] Christopher M. Colangelo,[5,6] Biff Forbush,[3] Clinton H. Joiner,[7] Erol E. Gulcicek,[5,6] Patrick G. Gallagher,[2] and Richard P. Lifton[1,5,*]
[1]Department of Genetics, Howard Hughes Medical Institute
[2]Department of Pediatrics
[3]Department of Cellular and Molecular Physiology
[4]Department of Pharmacology
Yale University School of Medicine, New Haven, CT 06510, USA
[5]Yale/National Heart, Lung, and Blood Institute Proteomics Center
[6]Keck Biotechnology Resource Laboratory
Yale University, New Haven, CT 06511, USA
[7]Cincinnati Comprehensive Sickle Cell Center, Division of Hematology/Oncology, University of Cincinnati College of Medicine and Department of Pediatrics, Cincinnati Children's Hospital Medical Center, Cincinnati, OH 45229, USA
*Correspondence: richard.lifton@yale.edu
DOI 10.1016/j.cell.2009.05.031

SUMMARY

Modulation of intracellular chloride concentration ($[Cl^-]_i$) plays a fundamental role in cell volume regulation and neuronal response to GABA. Cl^- exit via K-Cl cotransporters (KCCs) is a major determinant of $[Cl^-]_i$; however, mechanisms governing KCC activities are poorly understood. We identified two sites in KCC3 that are rapidly dephosphorylated in hypotonic conditions in cultured cells and human red blood cells in parallel with increased transport activity. Alanine substitutions at these sites result in constitutively active cotransport. These sites are highly phosphorylated in plasma membrane KCC3 in isotonic conditions, suggesting that dephosphorylation increases KCC3's intrinsic transport activity. Reduction of WNK1 expression via RNA interference reduces phosphorylation at these sites. Homologous sites are phosphorylated in all human KCCs. KCC2 is partially phosphorylated in neonatal mouse brain and dephosphorylated in parallel with KCC2 activation. These findings provide insight into regulation of $[Cl^-]_i$ and have implications for control of cell volume and neuronal function.

INTRODUCTION

The establishment, maintenance, and modulation of the intracellular milieu play critical roles in diverse biological functions. One example is the dynamic regulation of intracellular Cl^- concentration ($[Cl^-]_i$), which plays a vital role in the maintenance of cell volume and modulation of the neuronal response to GABA.

Without a cell wall, eukaryotic cells face the threat of uncontrolled swelling and shrinkage from changes in extracellular osmolarity, which can rapidly result in cell death if unopposed. Diverse epithelia rigorously defend intracellular volume by rapidly activating electrolyte transport pathways to change intracellular solute concentration to prevent transmembrane water flux (Lang et al., 1998). This is primarily achieved by altering the balance between Cl^- entry and Cl^- exit via members of the SLC12A family of electroneutral cation-chloride cotransporters. These cotransporters can move Cl^- with or against its electrochemical gradient, using the large transmembrane gradients for Na^+ and K^+ (Figure 1). Cl^- influx occurs via the Na-K-Cl cotransporter NKCC1 (Lang et al., 1998) while Cl^- efflux occurs via the K-Cl cotransporters (KCC1–4) (Adragna et al., 2004; Gamba, 2005).

The activities of these cotransporters are coordinated and reciprocally regulated. Phosphorylation activates NKCC1 and inhibits KCCs, while dephosphorylation has opposite effects (Dunham et al., 1980; Jennings and Schulz, 1991; Altamirano et al., 1988; Lytle and Forbush, 1992; Haas and Forbush, 2000; Adragna et al., 2004) (Figure 1). The modulation of $[Cl^-]_i$ in response to osmotic challenge is rapid, occurring within minutes (Lang et al., 1998; Joiner et al., 2007). KCC activation in hypotonic stress is ablated by the phosphatase inhibitor calyculin A, suggesting an essential role of cotransporter phosphorylation in the acute response (Adragna et al., 2004). This homeostatic mechanism is widely conserved in species ranging from *Caenorhabditis elegans* to humans (Haas and Forbush, 2000; Adragna et al., 2004; Strange et al., 2006). While specific phosphorylation sites that account for NKCC1 regulation were identified by investigation in shark rectal gland, where expression is very high (Lytle and Forbush, 1992), the low abundance of KCCs has to date thwarted identification of their presumed regulatory phosphorylation sites.

In addition to their roles in cell volume regulation, NKCC1 and KCC cotransporters play a distinct role in neurons, determining $[Cl^-]_i$ and the response to γ-aminobutyric acid (GABA), the primary inhibitory neurotransmitter in the central nervous system

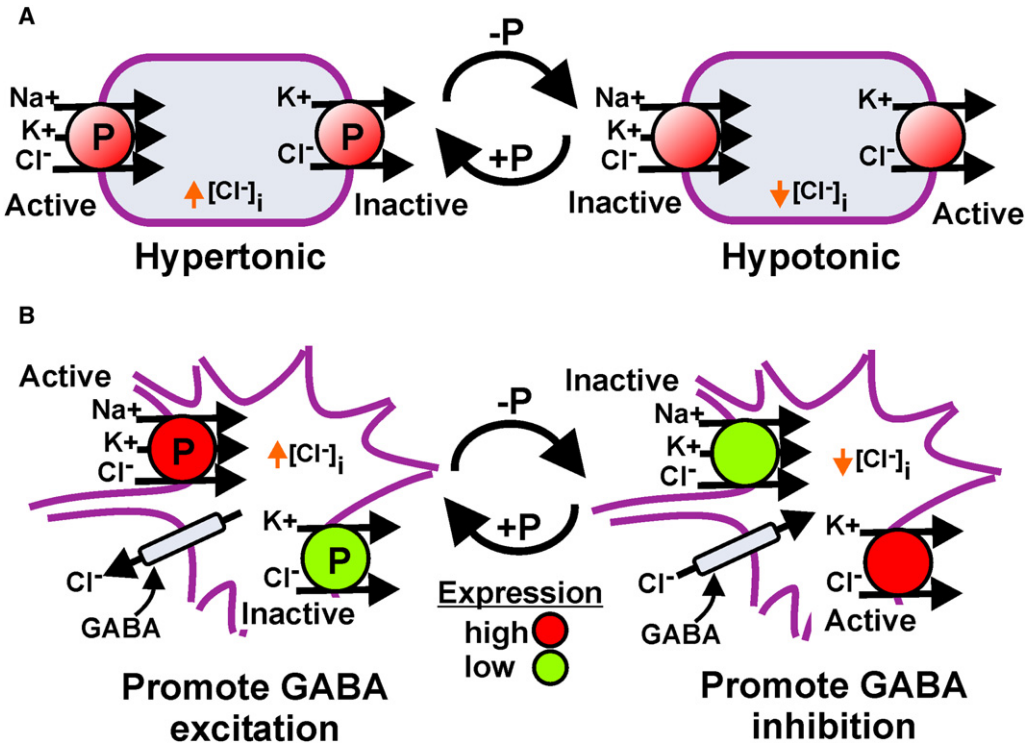

Figure 1. Chloride Cotransport Mechanisms in Cell Volume Control and Neuronal Response to GABA

Na-K-Cl and K-Cl cotransporters are depicted in a generic cell and neuron; their activities are believed to be reciprocally regulated by phosphorylation.

(A) Hypertonic conditions stimulate cotransporter phosphorylation (P) resulting in active Na-K-Cl cotransport and inactive K-Cl cotransport. Hypotonic conditions result in dephosphorylation, with inactive Na-K-Cl cotransport and active K-Cl cotransport.

(B) The balance between Na-K-Cl and K-Cl cotransport activities set the $[Cl^-]_i$ in $GABA_A$-positive neurons. $[Cl^-]_i$ and the membrane potential determines the flux of Cl^- in response to GABA. K-Cl cotransport expression increases and Na-K-Cl expression decreases postnatally.

(CNS). Binding of GABA to the $GABA_A$ receptor opens an associated Cl^- channel, $[Cl^-]_i$, and the membrane potential determines the resulting Cl^- flux, which in turn can modulate the response to GABA from hyperpolarization (inhibition) to depolarization (excitation). In the adult CNS, high KCC2 levels results in very low $[Cl^-]_i$ and GABA signaling results in inhibition in most neurons (Thompson and Gähwiler, 1989; Rivera et al., 1999). Conversely, in early development, NKCC1 levels are high while KCC2 activity is low, resulting in high $[Cl^-]_i$ and an excitatory response (Plotkin et al., 1997; Yamada et al., 2004). In rodent hippocampus, for example, this developmental switch from GABA excitation to inhibition occurs in the first week after birth (Rivera et al., 1999); however, there is heterogeneity in the timing of this switch (Ben-Ari, 2002). While KCC2 levels change in this time period, it is not clear that expression level alone, versus altered regulation of transporter activity, explains the increase in KCC2 activity. Similarly, some neurons in the adult, such as those in the suprachiasmatic nucleus, dynamically modulate $[Cl^-]_i$ and the response to GABA cycles from excitatory to inhibitory (Wagner et al., 1997). Moreover, prolonged postsynaptic spiking in mature neurons results in Ca^{2+}-dependent reduction in KCC2 activity, thereby reducing the inhibitory effect of GABA, which also occurs in a time frame not likely mediated by altered gene expression (Fiumelli et al., 2005). Finally, genetic deficiency for *KCC2* in mouse is postnatal lethal owing to disturbances in $[Cl^-]_i$ (Hübner et al., 2001).

In addition, K-Cl cotransport activity is prominent in reticulocytes and represents the major volume-sensitive cation transport mechanism in human erythrocytes (Brugnara and Tosteson, 1987; Brugnara et al., 1993). In sickle cell anemia, increased KCC activity results in increased Hb concentration, promoting Hb S polymerization (Brugnara et al., 1986; Eaton and Hofrichter, 1990; Lew and Bookchin, 2005; Joiner et al., 2007).

Efforts to identify regulatory sites on KCCs have heretofore been hampered by technological challenges that may be overcome by recent advances. Recently developed matrices such as titanium dioxide (TiO_2) can quantitatively bind and enrich phosphopeptides (Pinkse et al., 2004; Bodenmiller et al., 2007). Similarly, monitoring quantitative changes in phosphorylation has advanced with stable isotope labeling of amino acids in cell culture (SILAC) and multiple reaction monitoring (MRM), allowing direct comparison and precise quantitation of phosphopeptide levels in different experimental conditions (Ong et al., 2002; Olsen et al., 2006; Wolf-Yadlin et al., 2007).

Using these technologies, we now report the identification of two key phosphorylation sites, conserved among all KCC isoforms, which regulate KCC activity and are modulated across development and by physiologic perturbation.

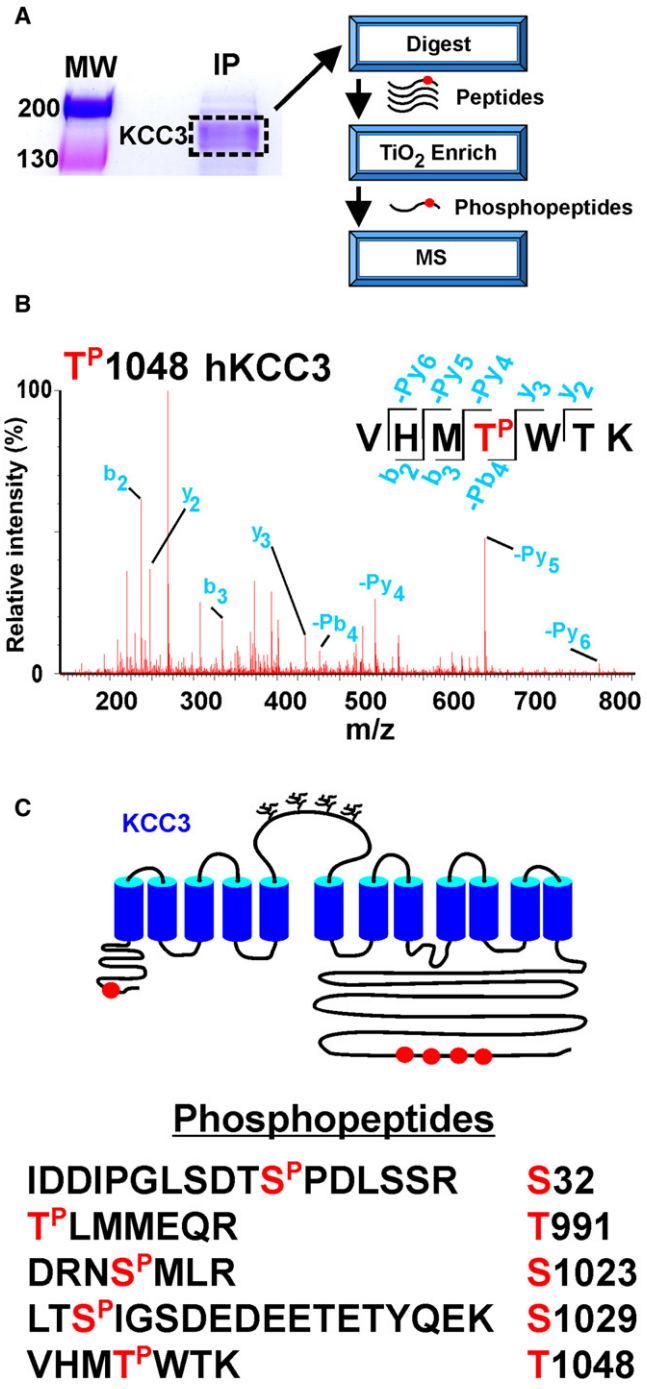

Figure 2. Identification of Phosphorylation Sites in KCC3

(A) Phosphorylation site mapping. Myc-tagged human KCC3 was purified and digested with trypsin and phosphopeptides were enriched on TiO_2 and subjected to LC-MS/MS.

(B) Representative MS/MS spectrum. Assignment of the peptide VHMT^{P}WTK (T^P1048) is shown. The phosphorylated precursor ion, 491.7 $^{+2}$, was selected and produced the fragment ion spectrum shown. Specific y and b fragment ions allowed unambiguous identification of the precursor peptide and phosphorylation at T1048. Fragment ions with neutral loss of phosphate ($-P_y4$, $-P_b4$, etc.) are indicated.

(C) Identified phosphorylation sites in KCC3. The topology of KCC3 is depicted and identified phosphorylation sites are indicated in red; the phosphopeptides identified are shown numbered as in human KCC3a (GeneID 9990). All KCC3 peptides observed are listed in Table S1.

RESULTS

Identification of KCC3 Phosphorylation Sites

We made a stable HEK293 cell line with tetracycline-regulated expression of human myc-tagged KCC3 inserted into a defined site in the genome as a single copy (HEK-KCC3^{tetON}). Clonal cell lines with tetracycline-inducible expression of KCC3 showed low levels of endogenous KCC activity, and transgenic KCC3 activity, as measured by ^{86}Rb uptake, showed the expected properties of tetracycline dependence, marked stimulation by extracellular hypotonicity, chloride dependence, sensitivity to 2 mM furosemide, and ablation of hypotonic stimulation by the phosphatase inhibitor calyculin A (see Figures S1 and S3 available online; data not shown).

To map phosphorylation sites on KCC3, we used phosphopeptide enrichment coupled to LC-MS/MS. KCC3 was purified by immunoprecipitation (IP) using anti-myc antibodies followed by SDS-PAGE, digested with trypsin, and applied to a matrix of TiO_2 (Figure 2A; Pinkse et al., 2004). Both TiO_2-bound and unbound fractions were separated on a C18 reverse phase nano-HPLC column and directly injected into an ESI-QTOF mass spectrometer.

From the MS/MS results, KCC3 phosphopeptides and non-phosphopeptides were identified using the Mascot database search algorithm, verified by manual inspection of the spectrum (Figure 2B) (Perkins et al., 1999). Peptides from the TiO_2-bound and unbound fractions covered ~77% of the amino acids of the N terminus and 59% of the C terminus of KCC3, including 65% of the serine and threonine residues in these segments. In contrast, we recovered only a small fraction of peptides from the remainder of the protein, which is highly hydrophobic with 12 predicted transmembrane domains (Figure S2 and Table S1).

In three mapping experiments we reproducibly observed the quantitative enrichment on TiO_2 of five phosphopeptides, with no phosphopeptides in the unbound fraction (Figures 2B and 2C and Table S1). All of these phosphopeptides and the sites of phosphorylation were unambiguously assigned from the precise match of the m/z ratio of observed peptide precursor ions and their fragment ions to those predicted to result from trypsin cleavage of KCC3. Phosphorylation sites were assigned from fragment ions bearing either the phosphate group itself or the signature of neutral loss of H_3PO_4 (−98 Da) (Figure 2B).

Reduced Phosphorylation of T991 and T1048 in Hypotonic Conditions

Because dephosphorylation is believed to be a key step in the activation of KCCs in response to cell swelling (Jennings and Schulz, 1991), we determined whether phosphorylation at any of these sites changes in response to extracellular hypotonicity using SILAC (Ong et al., 2002; Olsen et al., 2006), which permits direct comparison of phosphopeptide abundance in isotonic

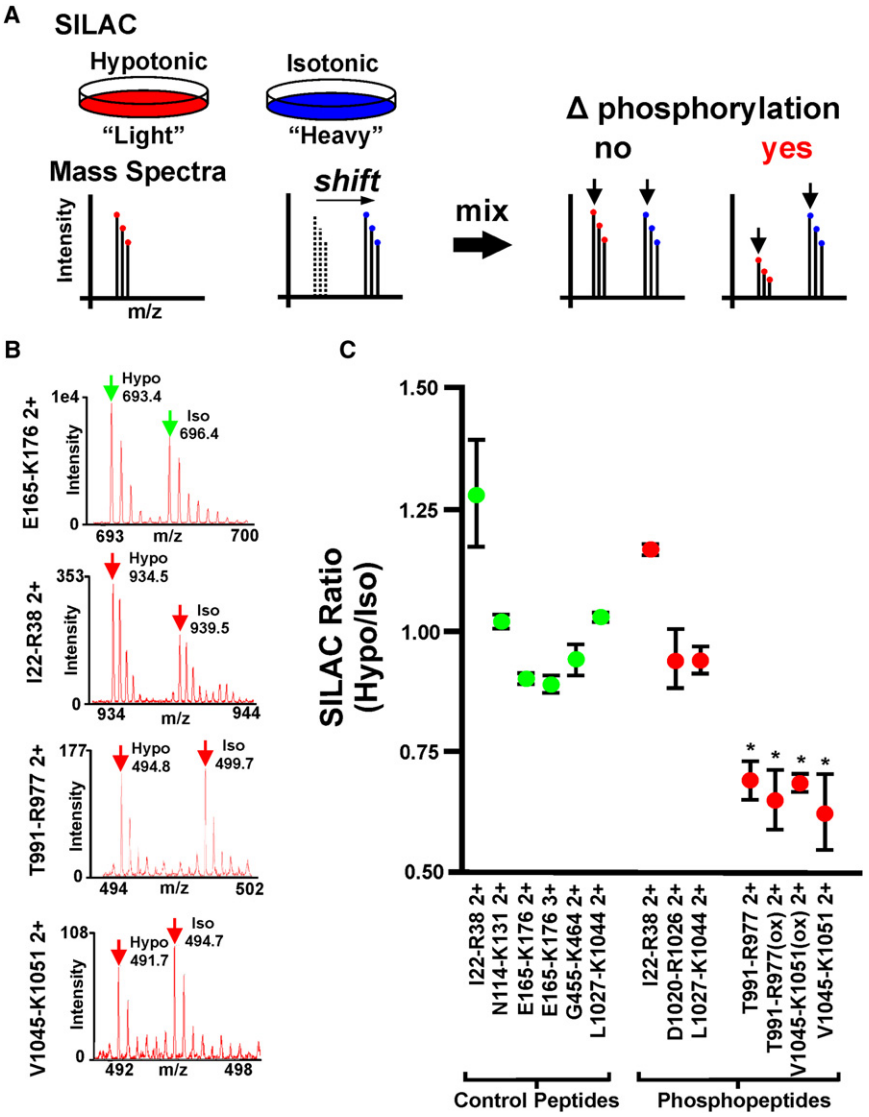

Figure 3. SILAC Analysis of KCC3 Phosphorylation Dynamics in Hypotonic Stress

(A) Schematic of SILAC experiment. HEK-KCC3^{tetON} were labeled with either "light" or "heavy" arginine and lysine and exposed for 5 min to either hypotonic or isotonic medium. Lysates from the two conditions were mixed and processed for identification of phosphopeptides.

(B) Representative MS spectra of SILAC pairs. The precursor ion spectra of nonphosphopeptide E165-K176^{+2} (SILAC pair 693.3/696.4) and the phosphopeptides I22-R38^{+2} (SILAC pair 934.2/939.3), T991-R977^{+2} (SILAC pair 494.7/499.7), and V1045-K1051^{+2} (SILAC pair 491.7/494.7) are shown. All SILAC pairs used for quantitation are listed in Table S1. Green arrows for control peptides and red arrows for phosphopeptides denote the peaks used for quantitation.

(C) The ratio of light to heavy m/z peak intensity (hypotonic to isotonic) of each peptide is presented as the mean ± SD of three biological replicates. Peptides are labeled per human KCC3a. I22-R38 (contains S^{P}32), D1020-R1026 (S^{P}1023), L1027-K1044 (S^{P}1029), T991-R997(T^{P}991), V1045-K1051(T^{P}1048).

and hypotonic conditions. HEK-KCC3^{tetON} was grown in either normal ("light") medium or "heavy" medium containing ^{13}C- and ^{15}N-labeled arginine (+10 Da) and ^{13}C-labeled lysine (+6 Da). The cells in heavy and light media were then exposed for 5 min to either isotonic (310 mOsm) or hypotonic (190 mOsm) medium, respectively (Figure 3A). Cells from each condition were lysed and mixed together; KCC3 was purified and applied to TiO_2 columns, and peptides bound to TiO_2 were quantitated by tandem MS following careful evaluation of the precursor ion spectra to ensure proper identification of each m/z peak of interest. The identities of all SILAC pairs were confirmed by identification of their fragment ions from MS/MS data. The heavy/light peptide ratios were obtained from the intensity of the first monoisotopic m/z peak of each precursor ion pair (Figure 3B).

In addition to the seven phosphopeptides queried (two phosphopeptides were recovered with both oxidized and unoxidized methionines), six acidic nonphosphorylated peptides of KCC3 that quantitatively bind to the TiO_2 matrix served as internal controls for each SILAC experiment.

The results of three biological replicates are shown in Figure 3C. The six control KCC3 peptides all gave consistent peptide ratios and there were no significant differences in the ratio among different peptides in this group. Comparison of all phosphopeptide ratios to all nonphosphopeptide ratios by ANOVA rejected homogeneity of all phosphopeptides and nonphosphopeptides ($p < 0.001$). Examination of the individual phosphopeptide ratios revealed that two phosphopeptides, bearing phosphorylation at T991 and T1048, showed significantly and reproducibly reduced phosphorylation in hypotonic conditions (35% reduction, $p = 0.00005$, and 33% reduction, $p = 0.00008$, versus nonphosphopeptide controls, respectively). Both the methionine-oxidized and nonoxidized forms of each of these two peptides showed reduced phosphorylation.

Dephosphorylation at T991 and T1048 Cooperatively Activate KCC3

The loss of phosphorylation at T991 and T1048 in hypotonic conditions suggests that dephosphorylation at these sites might be sufficient for activation of KCC3. We substituted alanine for threonine at these positions and also at S1023 as a control. These mutations were produced alone and in all possible pairwise combinations and were introduced into HEK293 cells as single copy transgenes and two independent clones of each mutant were studied. We induced expression of transgenic KCC3 and

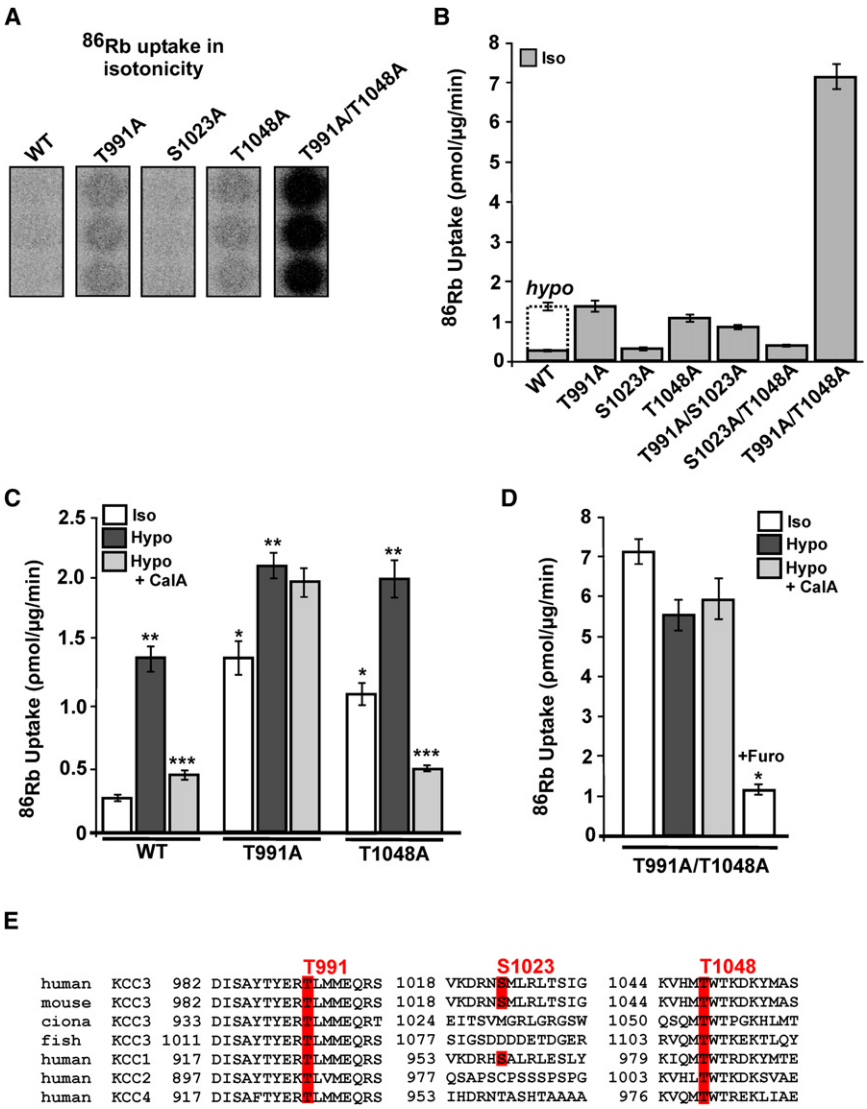

Figure 4. Alanine Substitutions at T991 and T1048 Cooperate to Activate KCC3

KCC3's harboring-indicated substitutions were engineered into HEK-KCC3^{tetON} and expressed and cells were exposed to ^{86}Rb in isotonic conditions.

(A) An autoradiogram showing ^{86}Rb uptake in cells in three individual wells demonstrates an increase in ^{86}Rb uptake in the T991A and T1048A single mutants and a dramatic increase in the T991A/T1048A double mutant.

(B) ^{86}Rb uptake in WT and mutant HEK-KCC3^{tetON} cells under isotonic conditions was quantitated and compared to values in WT cells exposed to hypotonic conditions. Mean ± SD of six independent flux experiments for each construct are shown for this panel and (C) and (D).

(C) ^{86}Rb flux assays in hypotonic conditions with and without calyculin A. The T991A and T1048A cell lines show further activation by hypotonic conditions (*$p \leq 0.00003$ versus wild-type (WT) flux in isotonicity; **$p \leq 0.00001$ for hypotonic versus isotonic conditions in each cell line; ***$p \leq 0.00004$ for the presence versus absence of calyculin A in hypotonicity in each cell line).

(D) The KCC3 T991A/T1048A double mutant (assayed as in C) is highly active in isotonicity (note change in scale compared to C), shows no further activation in hypotonic conditions, is insensitive to calyculin A (+CalA), and is inhibited by Furosemide (+Furo).

(E) Conservation of T991 and T1048 in KCC family members. The conservation of three phosphorylation sites is shown in KCC3 orthologues in mouse, sea squirt (*Ciona intestinalis*), green puffer fish, and human KCC1, 2, and 4. While S1023 is not conserved, T991, T1048, and their surrounding sequences are conserved among these and 31 other chordate KCCs (Acc# TF313657; http://www.treefam.org; Li et al., 2006).

assayed the resulting KCC-dependent ^{86}Rb uptake. KCC3 containing the single substitutions T991A or T1048A each showed highly significant increases in activity (4- to 5-fold, $p \leq 3 \times 10^{-9}$) in isotonic conditions in which the wild-type (WT) cotransporter shows little activity (Figures 4A and 4B). These activities are similar to those seen with hypotonic activation of the WT cotransporter (Figures 4B and 4C). In contrast, KCC3 with the S1023A substitution showed no significant change in activity. Combining either T991A or T1048A with S1023A showed no further increase in activity. However, combination of the T991A and T1048A substitutions resulted in a dramatic increase in KCC3 activity in isotonic conditions that was ~25-fold greater than activity of the WT cotransporter in isotonic conditions ($p < 3 \times 10^{-10}$; Figures 4A–4D). This activity was markedly greater than expected from simple additive effects of each mutant alone. Not surprisingly, cells expressing this constitutively active KCC3 become shrunken in isotonic conditions and begin to die if expression is maintained more than 16 hr (data not shown).

Exposure of cells with either the T991A or T1048A mutations to hypotonic conditions resulted in further increases in KCC activity (Figure 4C), suggesting that hypotonicity results in further dephosphorylation at the nonmutated site. Supporting this interpretation, KCC3 harboring both the T991A and T1048A substitutions does not increase activity in hypotonic conditions (Figure 4D), suggesting that no additional sites are involved in activation of cotransporter function.

The activation of KCCs in hypotonic conditions is mediated by protein phosphatases and is inhibited by calyculin A (Adragna et al., 2004). If the normal targets of these phosphatases are constitutively dephosphorylated (e.g., by mutation to alanine), calyculin A should be incapable of reverting KCC3 activation. The T991A/T1048A double mutant showed insensitivity to calyculin A (Figure 4D). Moreover, while the single mutant T991A could not be inhibited by calyculin A, the T1048A mutant was strongly inhibited (Figure 4C). These results suggest that T^{P}991 is the major target of the phosphatase inhibited by calyculin A.

Conservation of KCC3 Phosphorylation Sites and Candidate Kinases

Because hypotonic activation of KCCs is highly conserved (Adragna et al., 2004; Gamba, 2005), we evaluated the conservation of the identified phosphorylation sites and their contexts across 31 KCCs from 11 chordate species. Only T991 and T1048 are completely conserved in all orthologues and paralogues and lie in sequence motifs that are also highly conserved (Figure 4E).

To determine whether these identified phosphorylation sites correspond to known kinase specificities, we used PHOSIDA and NetworKIN algorithms (Olsen et al., 2006; Gnad et al., 2007). Interestingly, motifs at the highly conserved sites T991 and T1048 do not correspond to the specificity of any known kinase.

To determine whether the sites homologous to T991 and T1048 are phosphorylated in other KCC members, we developed antibodies specific for peptides that are phosphorylated at T991 and T1048 in KCC3 (Figure 5A). Signals from each phosphoantibody were specific, as they were abolished by treatment with alkaline phosphatase, phosphatase PP1A, or alanine substitution at these positions (Figure 5A). Because of the high degree of conservation of the immunizing peptide, these antibodies also recognize homologous phosphopeptides in human KCC1, 2, and 4; expression of these epitope-tagged KCCs followed by IP and western blotting show that KCC1, 2, and 4 are all phosphorylated at sites homologous to T991 and T1048 (Figure S3).

Hypotonicity Induces Dephosphorylation of KCC3 in Red Blood Cells

If T991 and T1048 play a role in the regulation of KCC3 in vivo, they should be phosphorylated in cells in which these cotransporters are inactive and dephosphorylated in conditions in which they are active.

Red blood cell KCC3 is maintained in a largely inactive state unless activated by hypotonic conditions. We purified native KCC3 and analyzed phosphopeptides by mass spectrometry (Figure 5B). We observed phosphorylation at both T991 and T1048 (Figure 5B and Table S2).

We next examined KCC3 phosphorylation dynamics in response to hypotonicity. Western blotting of KCC3 purified from red cells incubated in isotonic or hypotonic conditions demonstrated a reduction in phosphorylation at each site in response to hypotonicity. Quantitation of these signals in multiple biological and technical replicates suggests ~40% reduction in phosphorylation at each site (Figure 5C), consistent with results in HEK293 cells.

Dephosphorylation of Regulatory Sites Activates KCC3 Already Present at the Plasma Membrane

These findings raise the question of whether dephosphorylation increases the intrinsic transport activity of KCC3 that is already present at the plasma membrane or, alternatively, whether dephosphorylation is the trigger for translocation of KCC3 to the cell surface. To address this question we biotinylated cell surface proteins in KCC3-expressing HEK293 cells grown in isotonic conditions, purified biotinylated and nonbiotinylated fractions, and performed western blotting (Figure 6A). The results demonstrate that a large fraction of KCC3 is present at the plasma membrane in isotonic conditions and that this fraction is in fact enriched for KCC3 phosphorylated at T991 and T1048. These findings demonstrate that dephosphorylation is not required for KCC3 to reach the plasma membrane and supports a mechanism in which dephosphorylation increases KCC3's intrinsic transport activity.

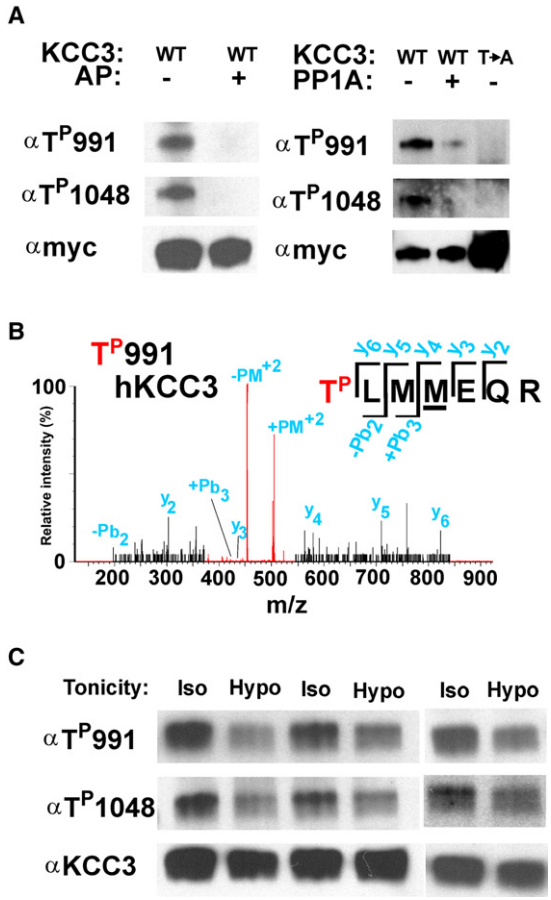

Figure 5. Phosphorylation of T991 and T1048 in KCC3 from Human Red Blood Cells and Response to Hypotonicity

(A) KCC3 phosphorylation detected via phosphospecific antibodies. WT myc-tagged KCC3 was purified and subjected to western blotting using antibodies specific for T^P991 or T^P1048 before and after treatment with alkaline phosphatase (AP), with PP1A, or in the presence of the T991A or T1048A substitutions. Blots were stripped and reprobed for total KCC3 with anti-myc antibodies.

(B) Endogenous KCC3 was purified from human red blood cells and phosphopeptides were identified after TiO_2 enrichment. A representative MS/MS spectrum from the phosphopeptide-containing T^P991 (precursor ion 502.7^{+2}) is shown. The precursor ion ($+PM^{+2}$) and the ion derived from neutral loss of the phosphate ($-PM^{+2}$) are observed (red spectra); other fragment ions (y and b ions) observed at lesser intensity in the same spectrum (black spectrum amplified 16-fold) confirm the identity of the precursor ion.

(C) KCC3 phosphorylation dynamics in response to hypotonic conditions. Human red blood cells were incubated in isotonic or hypotonic medium, KCC3 was isolated, and the level of KCC3 phosphorylation at T^P991 and T^P1048 from each treatment group was visualized by western blot using phosphospecific antibodies. The results show reduced phosphorylation at T991 and T1048 after exposure to hypotonic conditions.

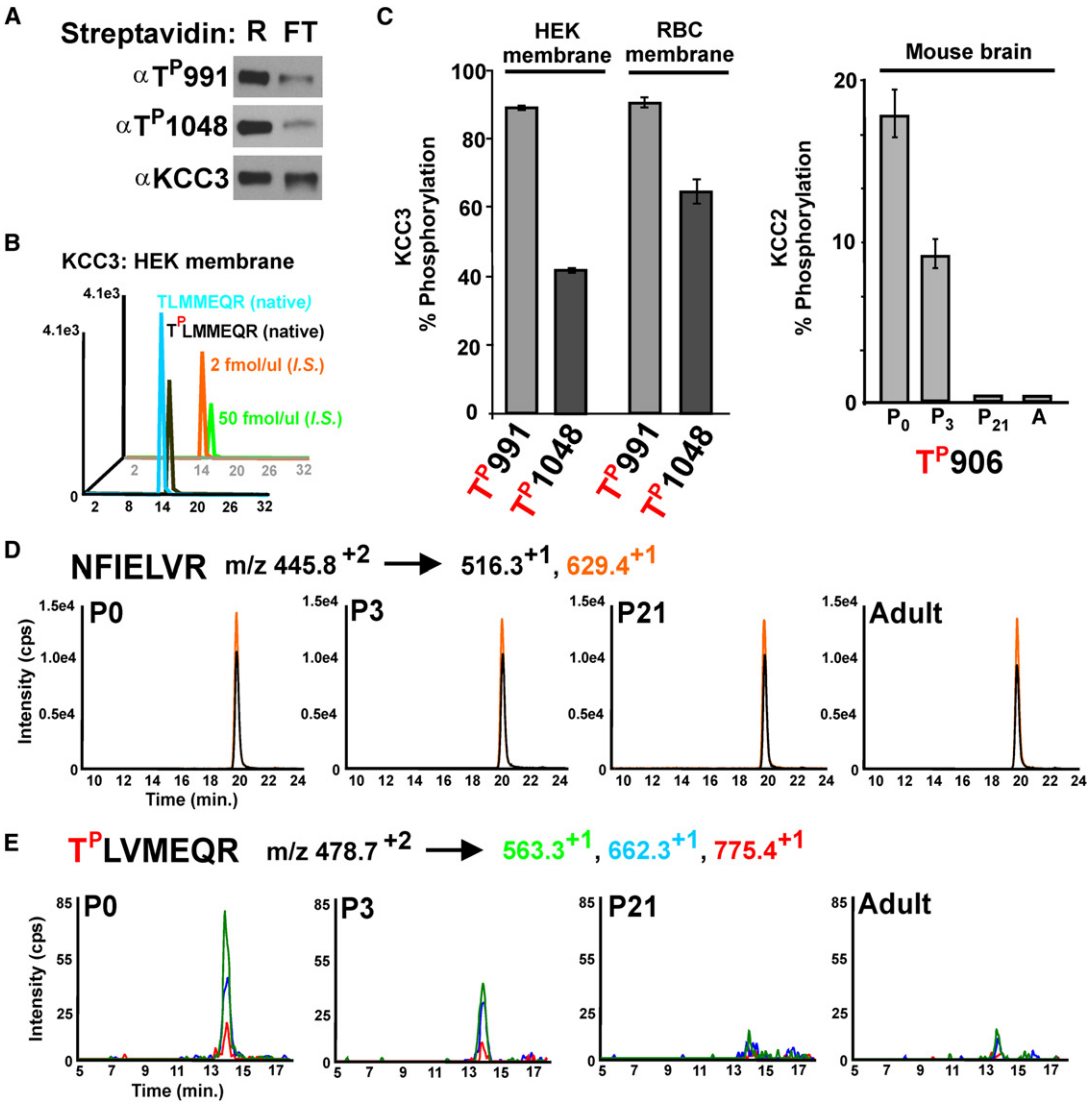

Figure 6. Localization, Dynamics, and Quantitation of KCC Phosphorylation In Vivo

(A) Western blot analysis of cell surface KCC3 in HEK^{tetON} cells. After cell surface biotinylation, biotinylated (R) and nonbiotinylated (FT) KCC3 proteins were purified. Equal volumes of each sample were compared on parallel blots and probed with antibodies to total (αKCC) or phospho-KCC3 (αT^{P}991 and αT^{P}1048). Phosphorylation at T^{P}991 and T^{P}1048 is greater in the surface pool of KCC3.

(B) MRM of KCC3 peptides from the HEK^{tetON} cell surface. MRM of the KCC3 peptides T^{P}LMMEQR (m/z 494.7^{+2}) and TLMMEQR (m/z 454.7^{+2}) were selected and y4 fragment ions (m/z 563.3^{+1} for each) were monitored. The extracted ion chromatograms of the native peptides and their corresponding internal standards are shown.

(C) Quantitation of KCC phosphorylation. Total phosphopeptide and nonphosphopeptide were calculated from the concentration curve obtained via MRM from the heavy labeled peptides (Figure S5). The mean and standard deviations are plotted for percent phosphorylation at the indicated site and were derived from quantities calculated from three separate fragment ions from each peptide.

(D) In vivo phosphorylation and developmental dynamics of mouse brain KCC2. MRM of a nonphosphorylated KCC2 peptide, NFIELVR (m/z 445.8^{+2}), from equal amounts of KCC2 protein at four developmental time points. Two fragment ions, m/z 516.3^{+1} and 629.4^{+1}, were monitored. Extracted ion chromatograms for these two fragment ions are shown, showing little difference in the amount of peptide across these time points.

(E) MRM of the KCC2 peptide T^{P}LVMEQR. The precursor ion T^{P}LVMEQR, m/z 478.7^{+2}, was selected. Three fragment ions, m/z 563.3^{+1}, 662.3^{+1}, and 775.4^{+1}, were monitored and their extracted ion chromatograms are shown, demonstrating nearly complete loss of all transitions of this phosphopeptide at later developmental stages.

Stoichiometry of Phosphorylation at Regulatory Sites

If KCC3 is present but inactive at the cell surface in isotonic conditions, these sites should be phosphorylated with high stoichiometry. MRM permits determination of the absolute stoichiometry of phosphorylation at these sites by introducing known amounts of heavy isotope-labeled synthetic peptides corresponding to their phosphorylated and nonphosphorylated versions, generating a standard curve, and then quantitating

the experimentally observed amounts of each peptide. We purified cell surface-biotinylated KCC3 from HEK293 cells and KCC3 from human red blood cell ghost membrane preparations maintained in isotonic conditions and performed MRM. Consistent with expectations, the results demonstrate 89% phosphorylation at T991 and 42% phosphorylation at T1048 in HEK293 cells and 91% phosphorylation at T991 and 65% at T1048 in human red blood cells (Figures 6B and 6C).

Modulated Phosphorylation and Activity of KCC2 in Mouse Brain Development

Unlike red cell KCC3, which is inactive and highly phosphorylated at T991 and T1048 under basal conditions, neuronal KCC2 is normally highly active in adult brain, but there is little KCC2 activity in neonatal brain. We consequently would expect to find low phosphorylation of KCC2 in adult brain and higher phosphorylation in neonatal brain (accepting that additional factors such as lower gene expression in neonatal brain also play a role; Rivera et al., 1999). We purified endogenous KCC2 from mouse brain at P0 (the day of birth) and searched for KCC2 phosphopeptides and nonphosphopeptides by TiO_2 and MS/MS as above. At P0 we detected phosphorylation at positions T906 and T1006, homologous to the regulatory sites in KCC3 (Table S2 and Figure S5). In contrast, interrogation of these same two sites in adult brain showed no evidence of phosphorylation by this method.

To quantitate this developmental change, we performed MRM without TiO_2 enrichment. Equal amounts of KCC2 from different developmental time points (P0, P3, P21, and adult brain) were analyzed for phosphorylation at T906 and compared to levels of a nonphosphorylated control peptide and nonphosphorylated T906 (Figures 6D, S4, and S5). Phosphorylation at T906 was progressively reduced with time, with a 33% reduction by P3 and >90% reduction at P21 and adult (Figures 6C–6E and S4). These results were statistically significant and reproducible in biological replicates.

While regulatory phosphorylation sites are conserved in KCC2, this alone does not establish that their modulation regulates KCC2 activity. To test this, we introduced either WT human KCC2 or KCC2 in which the threonine at positions 906 and 1007 have been substituted with alanine into HEK293 cells and measured the resulting KCC-dependent ^{86}Rb uptake in isotonic conditions. Similar to KCC3, KCC2 with these alanine substitutions showed a 4-fold increase in activity compared with WT KCC2 (Figure S6). This finding establishes that phosphorylation of these sites regulates activity of both KCC2 and KCC3 and strongly suggests that modulation of phosphorylation at the conserved sites in KCC1 and 4 will modulate their activities as well.

MRM experiments were also performed to measure absolute stoichiometry of phosphorylation at T906 in KCC2 from mouse brain at different developmental stages (the peptide containing T1006 in KCC2 could not be assayed due to extremely low ionization efficiency, a result confirmed by use of synthetic peptides and MRM). At P0, 18% of KCC2 is phosphorylated at T906. This fraction is reduced to 9% by P3 and to undetectable levels from day 21 onward (Figures 6C–6E and S4). Because this stoichiometry represents phosphorylation in the whole brain, this finding cannot distinguish between 18% phosphorylation in each neuron expressing KCC2 at P0 versus complete phosphorylation in neurons in some brain regions and complete dephosphorylation in others (or any intermediate models); this consideration is relevant since regional variation in KCC2 activity has been reported (Ben-Ari, 2002).

WNK1 Is Required for Normal Phosphorylation of T991 and T1048 in KCC3

We have attempted to identify kinases and phosphatases involved in the modulation of phosphorylation at KCC3 T991 and T1048. We examined the ability of purified protein phosphatases PP1, PP2A, PP2B, and DUSP22 to dephosphorylate T^P991 and T^P1048 in KCC3. Both PP1 and PP2A dephosphorylated both sites, while the latter phosphatases did not (Figure S3).

The WNK kinases and SPAK/OSR1 are strong candidates for KCC3 regulatory kinases. The WNK kinases play a role in the orchestration of activities of the SLC12A family of electroneutral cotransporters (Kahle et al., 2005; Rinehart et al., 2005; de Los Heros et al., 2006), and the kinase activity of WNK1 is modulated by changes in extracellular tonicity (Xu et al., 2000; Wilson et al., 2001; Strange et al., 2006). Similarly, the kinases SPAK and OSR1 play a role in modulation of NKCC1 activity (Vitari et al., 2006). By quantitative PCR of the HEK-KCC3^{tetON} cells, we found robust expression of *WNK1* and *SPAK*, with lower levels of *OSR1*, still lower levels of *WNK2*, and orders of magnitude lower expression of *WNK3* and *WNK4* (data not shown).

We used RNA interference (RNAi) to individually knock down expression of each of these six genes in HEK-KCC3^{tetON} cells. For each gene, at least two small-interfering RNA (siRNA) duplexes that individually produce $\geq$75% knockdown of the target were identified and assayed in at least three biological replicates. After 24 hr exposure to siRNAs, KCC3 expression was induced for 16 hr and phosphorylation at T991 and T1048 was examined by western blotting (Figure 7A). siRNAs targeting *KCC3* demonstrated robust knockdown of KCC3 protein, providing a positive control, and random sequence negative controls as well as siRNA for the low-level expressed *WNK2*, *3*, and *4*, did not change phosphorylation at T991 and T1048 (Figure 7B). Similarly, knockdown of *SPAK* and *OSR1* had no significant effect on T991 or T1048 phosphorylation (data not shown). In contrast, knockdown of *WNK1* with either of two siRNAs reproducibly reduced phosphorylation at both T991 and T1048 (Figures 7C and 7D), implicating WNK1 in the regulation of phosphorylation at these sites.

DISCUSSION

We have identified phosphorylation sites in KCCs that regulate their activities. High degrees of phosphorylation at these sites inhibit activity at the plasma membrane and mutations that prevent phosphorylation at these sites result in dramatic constitutive activation. The physiologic relevance of regulated phosphorylation at these sites for the acute response to hypotonic stress seems clear since both HEK293 and human red blood cells have high stoichiometric phosphorylation of these site in isotonic conditions in which KCC activity is low, and these sites are rapidly dephosphorylated in response to hypotonic stress,

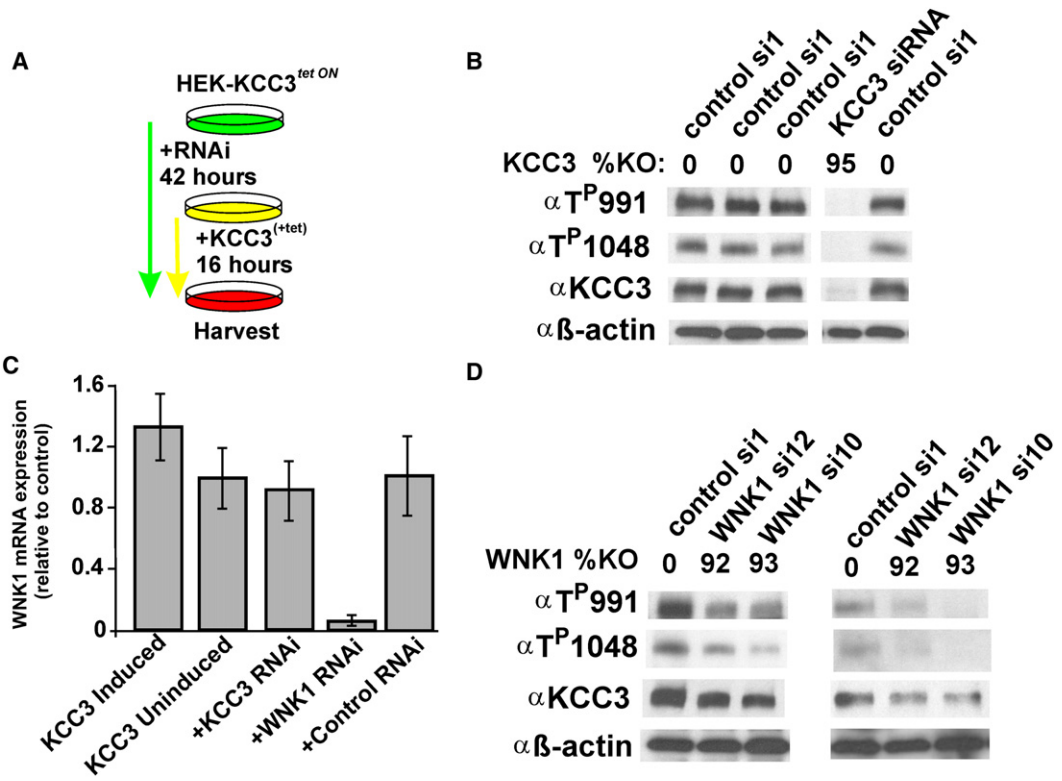

Figure 7. RNAi Targeting of WNK1 Reduces KCC3 Phosphorylation

(A) RNAi experimental scheme. siRNAs were introduced into HEK-KCC3^{tetON} cell lines by transient transfection. KCC3 expression was induced 24 hr later, lysates were harvested after 16 hr, and KCC3 phosphorylation was examined by western blot with phosphoantibodies for T^{P}991 and T^{P}1048.

(B) Experiments with control siRNAs and siRNAs targeting *KCC3* are shown and demonstrate stability of negative controls and utility of positive controls.

(C) Quantitative PCR assays of *WNK1* expression. *WNK1* transcripts were assayed via gene-specific TaqMan reagents and show specific knockdown in the presence of *WNK1* siRNAs (mean and standard deviation of six replicate experiments for each group; the *WNK1* siRNA group is pooled data from the two different siRNAs used).

(D) Reduced phosphorylation at T991 and T1048 after reduction of *WNK1* expression. Lysates from HEK-KCC3^{tetON} cell lines transfected with *WNK1*-specific or control siRNA were analyzed for phosphorylation at T991 and T1048 by western blotting. The percentage of reduction in *WNK1* expression in each experiment is indicated for biological replicate experiments and the results of western blotting using two different *WNK1* siRNAs are shown. The results demonstrate reduced phosphorylation at T991 and T1048 after *WNK1* knockdown.

paralleling induction of transport activity. In developing brain, the phosphorylation state of KCC2 parallels KCC2 activity, with virtually complete dephosphorylation in adult, where KCC2 activity is maximal. This observation suggests that modulated phosphorylation at these sites may play a role in regulation of $[Cl^-]_i$ in GABA-responsive neurons, complementing other regulatory mechanisms such as protein turnover and gene expression (Rivera et al., 2004; Lee et al., 2007); nonetheless, further work will be required to directly assess the physiologic role of KCC2 phosphorylation.

These findings provide insight into the regulation and modulation of $[Cl^-]_i$ by KCCs and highlight the ability of targeted quantitative phosphoproteomics to provide important insight into biological regulation as well as biomarkers and reagents to probe and assess functional states. Measurement of phosphorylation at these sites may prove a useful biomarker for assessing the state KCC3; for example, increased KCC3 activity is believed to contribute to sickle crisis in patients with sickle cell anemia. Moreover, these findings provide a means for producing constitutively active KCC3 and it will be of interest to determine the effects of constitutively active KCC3 expressed in red blood cells and other tissues in vivo. Similarly, these findings suggest a testable mechanism for the acute inhibition of KCC2 activity that has been observed to occur in response to prolonged post-synaptic spiking and is believed to be phosphorylation dependent (Fiumelli et al., 2005). Finally, it will also be of interest to determine the correlation of phosphorylation at regulatory sites in KCC2 with response to GABA in brain nuclei that are known to regularly modulate their response to GABA (Wagner et al., 1997).

These findings provide further opportunities to define both the upstream signaling pathway that regulates KCCs as well as the molecular mechanisms of their activation. Knockdown of *WNK1* via RNAi supports a role for this kinase in the maintenance of phosphorylation at these sites. This could occur either via direct phosphorylation of KCC3 by WNK1 or via activation of other kinases that act at these sites. Alternatively, WNK1 could negatively regulate phosphatase activity, and loss of WNK1 effects would activate the phosphatase that acts at these sites.

The identification of these regulatory sites provides important tools that will enable elucidation of the signaling pathways that regulate KCC activities.

The sequence context of T991 is similar to a motif found in the N terminus of the SLC12A cotransporter NKCC1 and which is involved in its regulation (Darman and Forbush, 2002; Dowd and Forbush, 2003; Vitari et al., 2006; Gagnon et al., 2007). This motif, YXRT^{P}, could be phosphorylated by a single kinase that positively regulates KCC3 and negatively regulates NKCC1 (Figure S7), consistent with the expectation that the same kinase might have opposing effects on the Cl^- entry and exit steps. Systematic mutagenesis of these sites in KCC3 and NKCC1 and assessment of the resulting transport activities will be required to assess this possibility.

The presence of two phosphorylation sites that have synergistic effects on KCC activity potentially allows regulation of KCC activity by different signals as well as modulation of the level of activity over a wider range than might be achieved by varying levels of phosphorylation at a single site. The nonadditive effects of the two sites further raises the question of whether dephosphorylation at each site is independent and stochastic or alternatively cooperative, with dephosphorylation at one site promoting dephosphorylation at the second.

Similarly, the molecular mechanisms that distinguish inactive from active KCCs have been poorly understood. Our results do not support a model in which dephosphorylation is required for translocation of KCC3 to the plasma membrane and instead suggest that dephosphorylation increases intrinsic transport activity. As a consequence, our findings should permit testing of homogenous forms of KCCs in relevant models as either constitutively active or inactive forms, enabling comparison of their biochemical and biophysical properties as well as the identification of proteins that may be physically associated with these alternative forms.

Finally, these studies also provide tools for probing the phosphorylation of these sites and KCC function in vivo. These may prove relevant to understanding diverse physiologic processes including cell growth and volume control, normal and abnormal neuronal and CNS functions, pathophysiology of sickle cell disease, and electrolyte homeostasis. Further understanding of the regulation of phosphorylation at these sites may provide opportunities for their selective modulation for health benefit.

EXPERIMENTAL PROCEDURES

Sources of KCC Proteins

HEK293 Cells

Single copies of WT or mutant human *KCC3a* cDNAs with an N-terminal *myc* epitope expressed under tetracycline control were introduced into HEK293 cells using the Flp-in T-Rex System (Invitrogen). KCC3 was induced at 50% confluence with tetracycline for 16 hr. Cells were disrupted with a syringe and narrow gauge needle on ice in the presence of protease and phosphatase inhibitors in Triton X lysis buffer (TX-LB).

Human Red Blood Cells

Venous human blood was collected from healthy adults, washed, and lysed. Red cell membrane "ghosts" were prepared by centrifugation and proteins were extracted with TX-LB and used for IP.

Mouse Brain

Whole mouse brains (P0, six brains; P2, approximately three to four brains; P7, P21, and adult, two brains per IP) were collected immediately after sacrifice, dissected on ice, homogenized in TX-LB, and centrifuged, and the supernatant was collected and used for IP.

IP and Purification of KCCs

Myc-tagged human KCC3 was purified from HEK-KCC3^{tetON} lysates using anti-myc antibodies. Native human KCC3 was purified from red cell membrane preparations using goat anti-KCC3. Native mouse KCC2 was purified from brain using rabbit anti-KCC2. Protein extracts were mixed with antibodies and IPs were collected, fractionated by SDS-PAGE, and visualized with Coomassie blue.

TiO_2 Enrichment and LC-MS/MS

Proteins of interest were excised from gels and digested with trypsin. Peptides were extracted with 0.5% trifluoroacetic acid, dried, resuspended, and applied to a TiO_2 TopTip micro-spin column (Glygen Corp.). Unbound peptides were washed off and bound peptides were eluted with a 1:33 solution of saturated ammonia. Protein digests and SILAC experiments were analyzed by LC-MS/MS. Identified sites of phosphorylation were confirmed using a second spectrometer. Spectra were searched with Mascot 2.1 with improved phosphopeptide scoring. Phosphopeptide identities were confirmed by manual inspection.

Phosphatase Assays and Immunoblotting

Purified myc-tagged KCC was dephosphorylated by incubation with alkaline phosphatase, PP1A, PP2A, PP2B, or DUSP22 for 60 min at 30°C and subjected to western blotting with anti-myc and phosphospecific antibodies $\alpha T^{P}991$ and $\alpha T^{P}1048$, followed by imaging with ECL reagents (GE Healthcare) and autoradiography.

Quantitative Comparisons in Cell Cultures with SILAC

SILAC Labeling and Protein Preparation

WT HEK-KCC3^{tetON} cell lines were passaged at 10% confluence in heavy (L-lysine-$^{13}C_6$, and L-arginine-$^{13}C_6{}^{15}N_4$) or light (normal) SILAC media. Cells were grown to confluence and replated, still in heavy or light medium. KCC3 expression was induced at ~50% confluence and cells were cultured an additional 16 hr, after which heavy-labeled cells were incubated for 5 min in isotonic media while light-labeled cells were incubated for the same time in hypotonic media . Cells were then lysed in TX-LB as above. Proteins in each lysate were quantitated (BCA assay; Pierce) and equal amounts from heavy and light conditions were mixed together. KCC3 expression in each condition was similar as determined by western blotting. Myc-tagged KCC3 was then purified via IP as described above.

Quantitative Mass Spectrometry for SILAC

Immunoprecipitated, SILAC-labeled KCC3 proteins were purified and enriched with TiO_2 as above. SILAC data sets were acquired with LC-MS/MS as above with additional MASCOT searches to confirm SILAC-derived peptide pairs. The ratios of the heavy and light tryptic peptides were extracted manually from the average intensity values of the first monoisotopic m/z peak of all the mass spectra spanning the LC elution range of interest. All of the precursor peptide and phosphopeptide m/z values used in ratio determinations were confirmed to match the sequence of KCC3 by their MS/MS fragment spectra. Quantitation for each peptide was performed on three biological replicates. The mean values of the light/heavy intensity ratios of the six control nonphosphopeptides were normalized to a ratio of 1.0 and the ratios in phosphopeptides were adjusted by the same factor; use of non-normalized data does not change the significance of the results.

Quantitative Comparisons In Vivo with MRM

LC-MRM was performed using KCC2 from mouse brains of different developmental stages prepared for MS without TiO_2 enrichment. Samples were normalized to provide equal amounts of KCC2 for mass spectrometry. Transitions were selected from MS/MS data and refined with Applied Biosystems MRMPilot 0.9beta (Table S3). LC-MRM data was processed and quantitated by calculating the area under the extracted ion chromatogram using Applied Biosystems Multiquant 1.0 software. Data from Multiquant were exported and uploaded into the Yale Protein Expression Database (Shifman et al., 2007).

^{86}Rb Uptake Assays

Assays were performed with an automated flux system (Darman and Forbush, 2002). HEK-KCC3^{tetON} cell lines expressing WT or mutant KCC3 proteins were passaged to 50% confluence, and KCC3 was induced for 16 hr. For the KCC2 studies, the cotransporter was introduced via transient transfection (Lipofectamine 2000; Invitrogen) and assayed after 24 hr of protein expression. For flux assays, the medium was replaced with isotonic or hypotonic medium for 6 min. Cells were then incubated for 2 min in regular flux media (Darman and Forbush, 2002), washed, dried, and exposed to phosphorimaging plates, scanned with a GE-Storm Phosphorimaging system, and quantitated with Imagequant software. After quantitation, total protein per well was determined. ^{86}Rb uptake was calculated as pmol/μg/min for each well. For calyculin A pretreatment, cells were exposed to calyculin A at room temperature for 10 min prior to initiation of the flux experiment. For furosemide inhibition studies, furosemide was added to the preincubation step and at the flux step.

Erythrocyte Osmotic Stress Studies

Human red blood cells were subjected to hypotonic stress (Joiner et al., 2007). Washed erythrocyte cell pellets were resuspended in either ~320 mOSM isotonic media or ~220 mOsm hypotonic media and incubated for 10 min at 37°C. Membranes were then prepared as above. Native KCC3 was immunopecipitated with goat anti-human KCC3. Membrane samples were normalized by mass and an equivalent amount of antibody per IP was used to ensure equivalent loading across treatment groups for western blot analysis.

RNAi Studies

siRNAs (Applied Biosystems) were introduced into HEK-KCC3^{tetON} cells via transient transfection. KCC3 phosphorylation was assayed after 42 hr of RNAi by western blotting.

Statistical Analysis

The Student's t test (two-tailed) was used to assess significance of differences between two groups; ANOVA was used to assess significance of differences among more than two groups. All experiments were performed at least in biological triplicate and with a minimum of two technical replicates for each biological replicate.

SUPPLEMENTAL DATA

Supplemental Data include seven figures, four tables, and Supplemental Experimental Procedures and can be found with this article online at http://www.cell.com/supplemental/S0092-8674(09)00634-5.

ACKNOWLEDGMENTS

We thank Terence Wu, Janet Crawford, Mary LoPresti, and Tom Abbott for their help and Christian Collin-Hansen and Angus Nairn for contributions to development of phosphoproteomics methods. This work was supported by National Heart, Lung, and Blood Institute (NHLBI) Proteomics Center N01-HV-28186 and National Institute on Drug Abuse (NIDA) 1P30DA018343, with instrumentation support from National Center for Research Resources (NCRR) UL1 RR024139 and 1S10RR024617-01 and HL65448 and DK62039 (P.G.G.); Cincinnati Comprehensive Sickle Cell Center U54HL07087 (C.H.J.) and GM083340 (B.F.); and the Leducq Transatlantic Network in Hypertension (R.P.L.). R.P.L. is an investigator of the Howard Hughes Medical Institute.

Received: August 7, 2008
Revised: December 29, 2008
Accepted: May 7, 2009
Published: August 6, 2009

REFERENCES

Adragna, N.C., Di Fulvio, M., and Lauf, P.K. (2004). Regulation of K-Cl cotransport: from function to genes. J. Membr. Biol. *201*, 109–137.

Altamirano, A.A., Breitwieser, G.E., and Russell, J.M. (1988). Vanadate and fluoride effects on Na+-K+-Cl- cotransport in squid giant axon. Am. J. Physiol. *254*, C582–C586.

Ben-Ari, Y. (2002). Excitatory actions of GABA during development: the nature of the nurture. Nat. Rev. Neurosci. *3*, 728–739.

Bodenmiller, B., Mueller, L.N., Mueller, M., Domon, B., and Aebersold, R. (2007). Reproducible isolation of distinct, overlapping segments of the phosphoproteome. Nat. Methods *4*, 231–237.

Brugnara, C., and Tosteson, D.C. (1987). Cell volume, K transport, and cell density in human erythrocytes. Am. J. Physiol. *252*, C269–C276.

Brugnara, C., Bunn, H.F., and Tosteson, D.C. (1986). Regulation of erythrocyte cation and water content in sickle cell anemia. Science *232*, 388–390.

Brugnara, C., Kruskall, M.S., and Johnstone, R.M. (1993). Membrane properties of erythrocytes in subjects undergoing multiple blood donations with or without recombinant erythropoietin. Br. J. Haematol. *84*, 118–130.

Darman, R.B., and Forbush, B. (2002). A regulatory locus of phosphorylation in the N terminus of the Na-K-Cl cotransporter, NKCC1. J. Biol. Chem. *277*, 37542–37550.

de Los Heros, P., Kahle, K.T., Rinehart, J., Bobadilla, N.A., Vazquez, N., San Cristobal, P., Mount, D.B., Lifton, R.P., Hebert, S.C., and Gamba, G. (2006). Wnk3 bypasses the tonicity requirement for K-Cl cotransporter activation via a phosphatase-dependent pathway. Proc. Natl. Acad. Sci. USA *103*, 1976–1981.

Dowd, B.F., and Forbush, B. (2003). PASK (proline-alanine-rich STE20-related kinase), a regulatory kinase of the Na-K-Cl cotransporter (NKCC1). J. Biol. Chem. *278*, 27347–27353.

Dunham, P.B., Stewart, G.W., and Ellory, J.C. (1980). Chloride-activated passive potassium transport in human erythrocytes. Proc. Natl. Acad. Sci. USA *77*, 1711–1715.

Eaton, W.A., and Hofrichter, J. (1990). Sickle cell hemoglobin polymerization. Adv. Protein Chem. *40*, 63–279.

Fiumelli, H., Cancedda, L., and Poo, M.M. (2005). Modulation of GABAergic transmission by activity via postsynaptic Ca2+-dependent regulation of KCC2 function. Neuron *48*, 773–786.

Gamba, G. (2005). Molecular physiology and pathophysiology of electroneutral cation-chloride cotransporters. Physiol. Rev. *85*, 423–493.

Gagnon, K.B., England, R., and Delpire, E. (2007). A single binding motif is required for SPAK activation of the Na-K-2Cl cotransporter. Cell. Physiol. Biochem. *20*, 131–142.

Gnad, F., Ren, S., Cox, J., Olsen, J.V., Macek, B., Oroshi, M., and Mann, M. (2007). PHOSIDA (phosphorylation site database): management, structural and evolutionary investigation, and prediction of phosphosites. Genome Biol. *8*, R250.

Haas, M., and Forbush, B., 3rd. (2000). The Na-K-Cl cotransporter of secretory epithelia. Annu. Rev. Physiol. *62*, 515–534.

Hübner, C.A., Stein, V., Hermans-Borgmeyer, I., Meyer, T., Ballanyi, K., and Jentsch, T.J. (2001). Disruption of KCC2 reveals an essential role of K-Cl cotransport already in early synaptic inhibition. Neuron *30*, 515–524.

Jennings, M.L., and Schulz, R.K. (1991). Okadaic acid inhibition of KCl cotransport. Evidence that protein dephosphorylation is necessary for activation of transport by either cell swelling or N-ethylmaleimide. J. Gen. Physiol. *97*, 799–817.

Joiner, C.H., Rettig, R.K., Jiang, M., Risinger, M., and Franco, R.S. (2007). Urea stimulation of KCl cotransport induces abnormal volume reduction in sickle reticulocytes. Blood *109*, 1728–1735.

Kahle, K.T., Rinehart, J., de Los Heros, P., Louvi, A., Meade, P., Vazquez, N., Hebert, S.C., Gamba, G., Gimenez, I., and Lifton, R.P. (2005). Wnk3 modulates transport of Cl- in and out of cells: implications for control of cell volume and neuronal excitability. Proc. Natl. Acad. Sci. USA *102*, 16783–16788.

Lang, F., Busch, G.L., Ritter, M., Völkl, H., Waldegger, S., Gulbins, E., and Häussinger, D. (1998). Functional significance of cell volume regulatory mechanisms. Physiol. Rev. *78*, 247–306.

Lee, H.H., Walker, J.A., Williams, J.R., Goodier, R.J., Payne, J.A., and Moss, S.J. (2007). Direct protein kinase C-dependent phosphorylation regulates the cell surface stability and activity of the potassium chloride cotransporter KCC2. J. Biol. Chem. *282*, 29777–29784.

Lew, V.L., and Bookchin, R.M. (2005). Ion transport pathology in the mechanism of sickle cell dehydration. Physiol. Rev. *85*, 179–200.

Li, H., Coghlan, A., Ruan, J., Coin, L.J., Hériché, J.K., Osmotherly, L., Li, R., Liu, T., Zhang, Z., Bolund, L., et al. (2006). TreeFam: a curated database of phylogenetic trees of animal gene families. Nucleic Acids Res. *34*, D572–D580.

Lytle, C., and Forbush, B., 3rd. (1992). The Na-K-Cl cotransport protein of shark rectal gland. II. Regulation by direct phosphorylation. J. Biol. Chem. *267*, 25438–25443.

Ong, S.E., Blagoev, B., Kratchmarova, I., Kristensen, D.B., Steen, H., Pandey, A., and Mann, M. (2002). Stable isotope labeling by amino acids in cell culture, SILAC, as a simple and accurate approach to expression proteomics. Mol. Cell. Proteomics *1*, 376–386.

Olsen, J.V., Blagoev, B., Gnad, F., Macek, B., Kumar, C., Mortensen, P., and Mann, M. (2006). Global, in vivo, and site-specific phosphorylation dynamics in signaling networks. Cell *127*, 635–648.

Perkins, D.N., Pappin, J.C., Creasy, D.M., and Cottrell, J.S. (1999). Probability-based protein identification by searching sequence databases using mass spectrometry data. Electrophoresis *20*, 3551–3567.

Pinkse, M.W., Uitto, P.M., Hilhorst, M.J., Ooms, B., and Heck, A.J. (2004). Selective isolation at the femtomole level of phosphopeptides from proteolytic digests using 2D-NanoLC-ESI-MS/MS and titanium oxide precolumns. Anal. Chem. *76*, 3935–3943.

Plotkin, M.D., Snyder, E.Y., Hebert, S.C., and Delpire, E. (1997). Expression of the Na-K-2Cl cotransporter is developmentally regulated in postnatal rat brains: a possible mechanism underlying GABA's excitatory role in immature brain. J. Neurobiol. *33*, 781–795.

Rinehart, J., Kahle, K.T., de Los Heros, P., Vazquez, N., Meade, P., Wilson, F.H., Hebert, S.C., Gimenez, I., Gamba, G., and Lifton, R.P. (2005). WNK3 kinase is a positive regulator of NKCC2 and NCC, renal cation-Cl- cotransporters required for normal blood pressure homeostasis. Proc. Natl. Acad. Sci. USA *102*, 16777–16782.

Rivera, C., Voipio, J., Payne, J.A., Ruusuvuori, E., Lahtinen, H., Lamsa, K., Pirvola, U., Saarma, M., and Kaila, K. (1999). The K+/Cl- co-transporter KCC2 renders GABA hyperpolarizing during neuronal maturation. Nature *397*, 251–255.

Rivera, C., Voipio, J., Thomas-Crusells, J., Li, H., Emri, Z., Sipilä, S., Payne, J.A., Minichiello, L., Saarma, M., and Kaila, K. (2004). Mechanism of activity-dependent downregulation of the neuron-specific K-Cl cotransporter KCC2. J. Neurosci. *24*, 4683–4691.

Shifman, M.A., Li, Y., Colangelo, C.M., Stone, K.L., Wu, T.L., Cheung, K.H., Miller, P.L., and Williams, K.R. (2007). YPED: a web-accessible database for protein expression analysis. J. Proteome Res. *6*, 4019–4024.

Strange, K., Denton, J., and Nehrke, K. (2006). Ste20-type kinases: evolutionarily conserved regulators of ion transport and cell volume. Physiology (Bethesda) *21*, 61–68.

Thompson, S.M., and Gähwiler, B.H. (1989). Activity-dependent disinhibition. II. Effects of extracellular potassium, furosemide, and membrane potential on ECl- in hippocampal CA3 neurons. J. Neurophysiol. *61*, 512–523.

Vitari, A.C., Thastrup, J., Rafiqi, F.H., Deak, M., Morrice, N.A., Karlsson, H.K., and Alessi, D.R. (2006). Functional interactions of the SPAK/OSR1 kinases with their upstream activator WNK1 and downstream substrate NKCC1. Biochem. J. *397*, 223–231.

Wagner, S., Castel, M., Gainer, H., and Yarom, Y. (1997). GABA in the mammalian suprachiasmatic nucleus and its role in diurnal rhythmicity. Nature *387*, 598–603.

Wilson, F.H., Disse-Nicodème, S., Choate, K.A., Ishikawa, K., Nelson-Williams, C., Desitter, I., Gunel, M., Milford, D.V., Lipkin, G.W., Achard, J.M., et al. (2001). Human hypertension caused by mutations in WNK kinases. Science *293*, 1107–1112.

Wolf-Yadlin, A., Hautaniemi, S., Lauffenburger, D.A., and White, F.M. (2007). Multiple reaction monitoring for robust quantitative proteomic analysis of cellular signaling networks. Proc. Natl. Acad. Sci. USA *104*, 5860–5865.

Xu, B., English, J.M., Wilsbacher, J.L., Stippec, S., Goldsmith, E.J., and Cobb, M.H. (2000). WNK1, a novel mammalian serine/threonine protein kinase lacking the catalytic lysine in subdomain II. J. Biol. Chem. *275*, 16795–16801.

Yamada, J., Okabe, A., Toyoda, H., Kilb, W., Luhmann, H.J., and Fukuda, A. (2004). Cl- uptake promoting depolarizing GABA actions in immature rat neocortical neurones is mediated by NKCC1. J. Physiol. *557*, 829–841.